

# Endless Optical Polarization Control at 56 krad/s, Over 50 Gigaradian, and Demultiplex of 112-Gb/s PDM-RZ-DQPSK Signals at 3.5 krad/s

Benjamin Koch, *Student Member, IEEE*, Vitali Mirvoda, Helmut Griebner, *Member, IEEE*, Horst Wernz, David Sandel, and Reinhold Noé, *Senior Member, IEEE*

**Abstract**—In this paper, we present an field-programmable gate array-based automatic endless optical polarization control system, which drives a commercial LiNbO<sub>3</sub> polarization transformer. It is capable of tracking endless polarization changes of up to 56 krad/s with mean and maximum polarization errors of 0.077 and 0.197 rad, respectively. While tracking up to 50 krad/s, the system was likewise tested over >2 weeks with maximum polarization error of 0.195 rad during which time it tracked polarization changes of 50 Gigaradian. 112-Gb/s polarization-division multiplexed return to zero differential quadrature phase-shift keying transmission with direct detection and polarization scrambling up to 3.5 krad/s is also demonstrated.

**Index Terms**—Optical fiber communication, optical fiber polarization, quadrature phase-shift keying (QPSK).

## I. INTRODUCTION

TRANSMISSION systems with coherent polarization diversity detection require fast analog–digital converters and complex signal processing. This increases costs and power consumption, especially at higher bitrates, which is prejudicial to moving to future high-performance transmission systems. On the other hand, more basic transmission systems with direct detection can also benefit from polarization multiplexing when using optical demultiplex with automatic polarization control [1]–[4]. Optical polarization demultiplexing is generally bitrate independent and can be used in combination with many modulation formats. The automatic polarization controller must be endless and fast enough to track any change of the state of polarization (SOP). SOP changes are usually the result of fluctuating thermal and mechanical stresses in the fiber of the transmission link [5]. While manual handling of the fiber can cause only limited polarization changes within 100 ms [6], hitting a reel of dispersion compensating fiber with a steel ball can provoke SOP changing speeds of up to 75000 rotations per second

(471 krad/s) on the Poincaré sphere [7] due to the mechanical shock. Endless control means that the polarization control is never interrupted by voltage resetting, even if the tracked polarization moves around the Poincaré sphere many or an unlimited number of times. Because polarization-dependent outages typically last longer than a forward-error correction (FEC) frame, short glitches would already cause a large number of bit errors that could not be corrected by FEC. Hence, a guaranteed tracking speed with bounded polarization errors for arbitrary polarization trajectories is an essential attribute of polarization control systems.

Beginning with the first integrated-optical endless polarization control system realized in 1987, published in 1988 [8], tracking speed rose from ~0.1 rad/s [8] to presently 38 krad/s [9]. In 1992, a tracking speed of 4.9 krad/s has been demonstrated by tracking ten periods of one particular repetitive endless Poincaré sphere trajectory in 20 ms [10]. In 2009, a 12.6-krad/s speed was reported, while tracking seemingly finite rather than endless polarization changes [11]. To our knowledge, more high-speed optical polarization control experiments have not been reported by other authors. Tests of commercial devices have revealed far slower control system responses [6].

We have recently tracked endless and arbitrary polarization changes in a polarization-division multiplexed differential quadrature phase-shift keying (PDM-DQPSK) field trial at 0.8-krad/s speed [1], and from 0 °C to 70 °C [12] and 1505–1570 nm [9]. Among the remaining challenges for commercialization of this technology is a longer continuously tracked trajectory length (presently 3.8 Gigaradian [9]). Likewise, it is tempting to increase tracking speed (beyond 38 krad/s [9]).

## II. ENDLESS POLARIZATION CONTROL SETUP

As a polarization transducer, we use a commercial polarization transformer (EOSPACE). It contains a cascade of eight integrated-optical Soleil-Babinet compensators (SBCs), i.e., rotary wave plates with adjustable retardation, implemented in X-cut, Z-propagation LiNbO<sub>3</sub> (see Fig. 1). Their response time is well below 10 ns.

Orientation and retardation of each SBC section can be modified with two voltages  $V_1$  and  $V_2$ , which generate horizontal and vertical electrostatic fields, respectively, inside the waveguide. If  $V_1$  and  $V_2$  are suitably normalized, the orientation of the SBCs fast eigenmode  $2\vartheta$  is determined by  $\tan 2\vartheta = V_2/V_1$  and can be rotated endlessly in the  $S_1$ – $S_2$  plane. The retardation

Manuscript received September 1, 2009; revised December 18, 2009 and January 25, 2010; accepted January 26, 2010. Date of publication April 5, 2010; date of current version October 6, 2010. This work was supported in part by the Deutsche Forschungsgemeinschaft and Bundesministerium für Wirtschaft und Technologie.

B. Koch, V. Mirvoda, D. Sandel, and R. Noé are with the Department of Optical Communication and High-Frequency Engineering, University of Paderborn, Paderborn 33098, Germany (e-mail: koch@ont.upb.de; mirvoda@ont.upb.de; sandel@ont.upb.de; noe@upb.de).

H. Griebner and H. Wernz are with the Business Unit Networks, Ericsson GmbH, Backnang 71522, Germany (e-mail: helmut.griesser@ericsson.com; horst.wernz@ericsson.com).

Color versions of one or more of the figures in this paper are available online at <http://ieeexplore.ieee.org>.

Digital Object Identifier 10.1109/JSTQE.2010.2042033

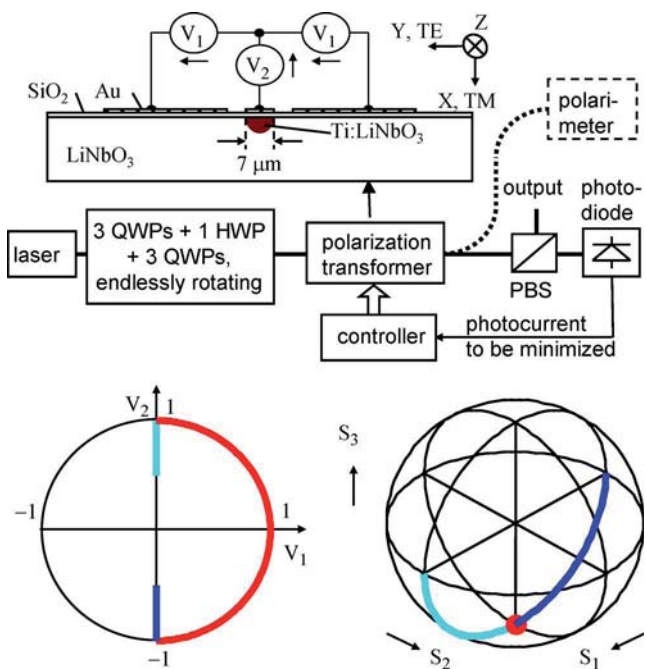


Fig. 1. (Top) Setup for endless polarization control with integrated-optical LiNbO<sub>3</sub> component containing eight electro-optic waveplates (SBCs). (Bottom) Trajectory in normalized voltage plane (left) capable of passing through circular polarization (right).

of the SBC is given by  $\varphi = \pi(V_1^2 + V_2^2)^{1/2}$  [8]. With a single SBC having a retardation  $\leq \pi$ , circular polarization can be transformed into any other polarization or *vice versa*. Voltages  $V_1 \sim \cos 2\vartheta$  and  $V_2 \sim \sin 2\vartheta$  are needed for a rotating wave plate. Here  $(d\vartheta/dt)/(2\pi)$  is the physical rotation frequency of an equivalent mechanical SBC, and  $(d2\vartheta/dt)/(2\pi)$  is the electrical rotation frequency (= eigenmode rotation frequency on the Poincaré sphere).

The gradient algorithm, implemented in a field-programmable gate array (FPGA), is likewise applicable for distributed polarization mode dispersion compensators in X-cut, Y-propagation LiNbO<sub>3</sub> [13]. In the following tracking experiments, it is used to stabilize the polarization-scrambled signal of an unmodulated laser source (see Fig. 1). A feedback signal, the relative intensity error (RIE), is generated by detecting one of the output signals of a polarization beam splitter (PBS) through which the signal is led after control. The algorithm seeks and reaches a global intensity minimum. At the same time, the other PBS output provides full intensity. At SBC section  $i$  (along the chip), the voltages  $V_{2i} \pm V_{1i}$  are applied. The RIE changes caused by small electrode voltage modulations yield partial derivatives. The operating points of the various voltages are modified in the direction of decreasing RIE toward a global minimum. Local minima do not exist, since enough complementary electrode voltages are available. If an electrode voltage reaches a limit given by the power supply rails, then, it is decreased in the following, while other voltages maintain correct control.

Indeed, controlling more than one wave plate simultaneously by the gradient algorithm reduces required voltages. It can be

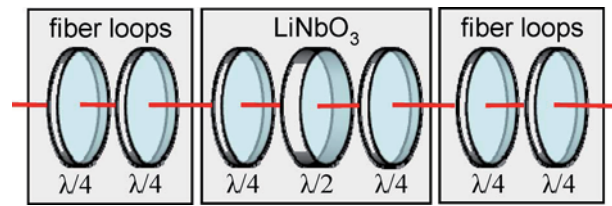


Fig. 2. Setup of HWP and six QWPs used for fast and endless polarization scrambling.

shown that with a large number of wave plates the fixed circular polarization needs no longer be fixed or circular. Rather, arbitrary generated polarization (at input) and analyzed polarization (at output) can be followed simultaneously. Even two wave plates are sufficient for this [14]. So, our usage of several wave plates greatly increases tolerance against device-inherent nonideal behavior and variations of the fixed output polarization and improves the reachable control speed.

More details on the control algorithm and device characterization process are given in [15].

### III. POLARIZATION SCRAMBLING SETUP

Great circles around the Poincaré sphere are most difficult to track for the polarization controller, because control voltages have to be kept inside their operational ranges. Most commercial polarization scramblers provide only limited back and forth polarization movements. To generate the fastest polarization changes on one endless polarization trajectory, a number of sections of a LiNbO<sub>3</sub> polarization controller device are driven as fast rotating wave plates. The driver board is the same, as for polarization control, but with a different FPGA configuration. A half-wave plate (HWP) is thereby placed between two quarter-wave plates (QWP) (see Fig. 2, middle).

Every electric revolution of the HWP generates two revolutions of the SOP around the sphere. Whenever there is linear polarization at the HWP input, the trajectory lies on a great circle and polarization-changing speed is maximized. At a 4-kHz electric rotation frequency of the HWP, polarization changes with 50 krad/s in this special case.

By placing a rotating QWP in front and behind the HWP, polarization circles at the output vary in sizes and orientations. The QWPs rotate at incommensurate rates between 60 and 70 Hz. Mean and rms scrambling speeds are  $\pi/4$  and  $(2/3)^{1/2}$  times the maximum speed, respectively.

Two pairs of rotating fiber loop QWPs running at rates between  $-6$  and  $+6$  Hz are also added to increase the randomness. In the following, the rotations of the QWPs are neglected in the calculation of the maximum polarization change speed. Fig. 3 shows the output polarization, which was recorded by a polarimeter. Rotation speeds were scaled down due to the limited polarimeter sampling speed (1 kHz).

For analysis purposes, the feedback signal is recorded in the FPGA. Fig. 4 shows the normalized feedback signal, i.e., the RIE with switched-OFF controller. Polarization rotations by  $2\pi$  with a frequency of 8 kHz can be observed, corresponding to

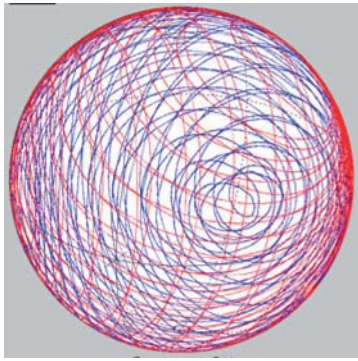


Fig. 3. Polarization trajectory generated by a HWP (1.6 Hz) between two QWPs (0.033 Hz and 0.021 Hz). Red and blue trace portions mean front and backside of Poincaré sphere, respectively.

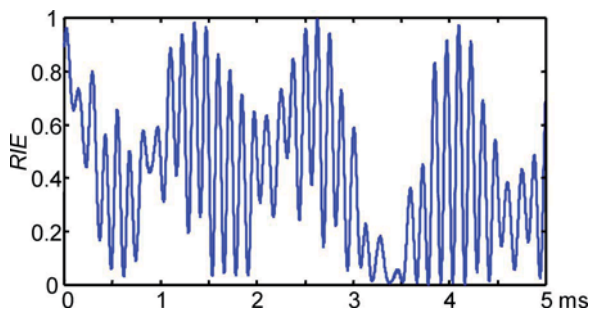


Fig. 4. RIE versus time for scrambled signal without polarization controller (HWP at 4 kHz, QWPs at 450 Hz and 230 Hz, generating up to 50 krad/s).

the HWP rotating at 4 kHz (electrical driving) for generating polarization changes up to 50 krad/s. For Fig. 4 only, the QWP speeds in LiNbO<sub>3</sub> were increased to 450 and 230 Hz. Otherwise Fig. 4 would have shown only little variations in amplitude and mean of the sine curve. But, the slower QWP speeds applied in the subsequent experiments may be considered to demonstrate control endlessness more convincingly.

Sampling is much faster than the generation of significant polarization changes in the scrambler, and happens upon polarization changes generated by the controller itself. While the measured RIE (=feedback signal) does not represent the true RIE, we believe that it is reasonably accurate. If noise and true RIE are statistically independent, then, the measured RIE and its limits surpassed with certain small probabilities are conservative estimates of the true RIE.

#### IV. HIGH-SPEED POLARIZATION CONTROL

Under control, the RIE, including the deviations caused by the voltage modulation, is recorded at about every 150 ns and put into a histogram. Histogram bins are added up to calculate the distribution function  $F(\text{RIE})$  of the RIE. Fig. 5 shows the complementary distribution function  $1-F(\text{RIE})$ , i.e., the probability that the RIE becomes worse than the value given on the abscissa. The traces show results of fourteen 30-min measurements at different maximum polarization changing speeds of 1, 10, 20, 30, 38, 40, 42, ..., 56 krad/s. For example, at 56 krad/s, an intensity loss of 0.67% is surpassed with a probability of

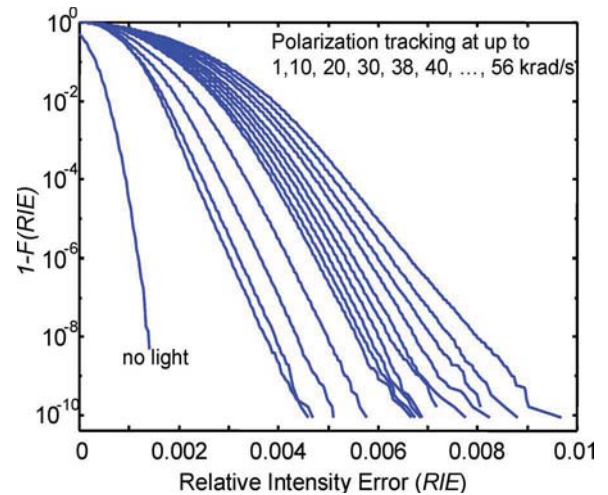


Fig. 5. Complementary distribution function  $1-F(\text{RIE})$  of RIE for different maximum polarization scrambling speeds. Each measurement lasted 30 min (except for the “no light” curve).

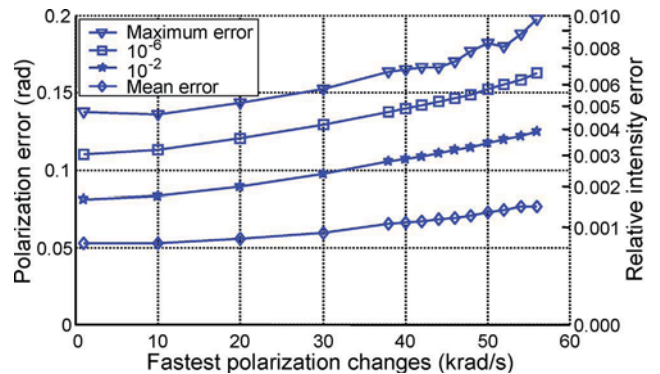


Fig. 6. RIE and polarization error, which are surpassed only with the given probabilities, as a function of scrambling speed.

$10^{-6}$ . The left-most trace shows a reference measurement without light to indicate measurement noise, and determine the point of zero intensity error ( $\text{RIE} = 0$ ).

Compared to the earlier setups [1], [9], [12], the clock speeds of the digital-analog converters (DACs) that generate the electrode voltages, and analog-digital converter (ADC) were doubled from 5 to 10 MHz. This allowed us to broaden the polarization dither spectrum. This measure improved maximum tracking speed and control quality at a given speed.

With the scrambler generating relatively slow polarization changes of up to 1 krad/s, mean and maximum RIE were measured to be 0.07% and 0.47%, respectively. At up to 38 krad/s, mean and maximum RIE were 0.11%, 0.675%, respectively. With maximally fast polarization changes of 56 krad/s, these errors were 0.15% and 0.97%, respectively.

Fig. 6 shows the RIE and derived polarization error of the tracking experiments for various thresholds of the complementary distribution function. The mean and maximum polarization errors are 0.065 and 0.164 rad at up to 38 krad/s, and 0.077 and 0.197 rad at maximum speed of 56 krad/s, respectively.

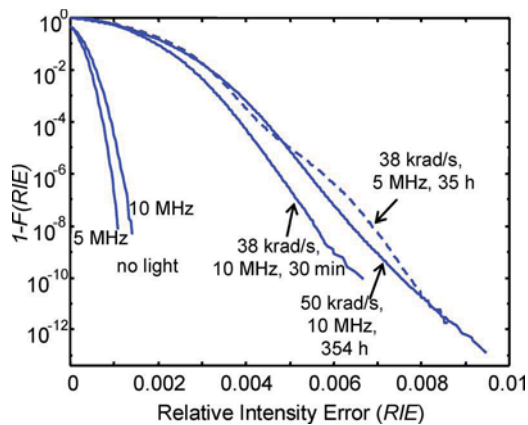


Fig. 7. Comparison of complementary distribution function  $1 - F(\text{RIE})$  of RIE for two long-term polarization tracking experiments with different DAC/ADC clock speeds.

From a control system point of view, the polarization variations are a ramp to be followed. An integral controller cannot track a ramp without residual error. In effect, it is the residual error, which drives the integrator to follow the ramp. For an integral controller, the residual ramp error is equal to the ramp slope times the  $1/e$  control time constant. The  $1/e$  control time constant indicates how fast the error caused by a polarization step decays. We apply this to our measurement results and estimate the control time constant with the help of the mean polarization error and the mean scrambling speed as  $0.077$  rad and  $(56 \text{ krad/s} \cdot \pi/4) = 1.75 \mu\text{s}$ , respectively. Since the electrode voltage dithering is likewise contained in the mean polarization error, this is a conservative guess.

Temperature ( $0^\circ\text{C}$ – $70^\circ\text{C}$ ) and wavelength ( $1505$ – $1570$  nm) insensitivity of the controller have recently been shown in [9], [12].

Limited by available time, the polarization controller was also tested at a scrambling speed of  $50 \text{ krad/s}$  in an unattended and uninterrupted experiment over  $354 \text{ h}$  ( $>2$  weeks). The tracked polarization trajectory is about  $50$  Gigaradian long. Fig. 7 shows the result and compares it to our previous long-term tracking experiment [9] at lower speed (dashed trace). The measurement noise increased (“no light” traces) due to the shorter measurement time at doubled ADC clock frequency. Maximum errors in the present  $50$ -krad/s experiment ( $0.95\%$ ,  $0.195$  rad) are slightly larger than the earlier at  $38 \text{ krad/s}$  ( $0.88\%$ ,  $0.188$  rad [9]). The small difference to the earlier (slower) experiment indicates that performance was improved. For direct comparison of the two setups, the  $38$ -krad/s trace of Fig. 5 is also shown in Fig. 7. The RIE threshold for an outage probability of  $10^{-10}$  is presently  $0.66\%$  while it used to be  $0.77\%$ . For a probability of  $10^{-2}$ , the RIE threshold decreased from  $0.32\%$  to  $0.28\%$ . Concurrently, the characteristic hump in the dashed trace, which showed up at tracking speeds greater than  $30 \text{ krad/s}$  in [9, Fig. 3]), disappeared.

## V. 112-Gb/s DQPSK POLARIZATION DEMULTIPLEXING

PDM-ASK transmission with direct detection and optical polarization control is possible [16], but suffers from optical non-

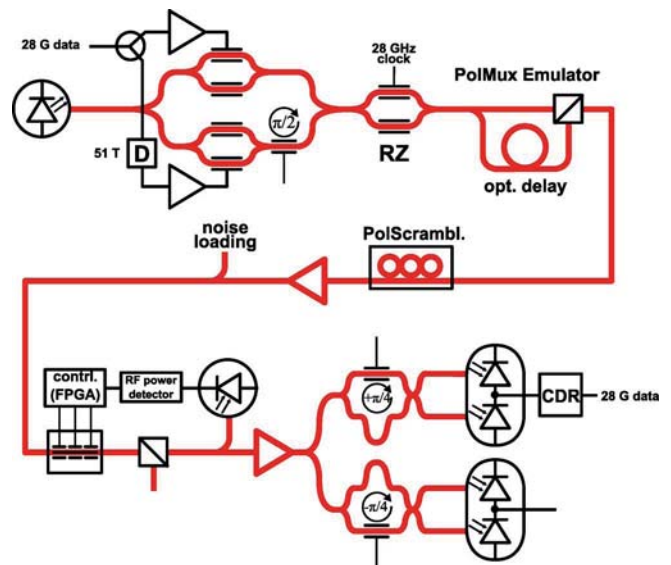


Fig. 8. PDM-RZ-DQPSK demultiplexing test setup with transmitter, polarization scrambler, polarization controller, and receiver.

linearity and achieves only medium spectral efficiency. Coherent PDM-QPSK systems are a candidate for  $100$ -GbE transmission with a channel spacing of  $50 \text{ GHz}$ . However, at the time of submission no real-time implementation for a coherent  $100$ -GbE receiver on a single carrier is available in the market [17]. Implementations based on two independent carriers double the number of optical components necessary. Furthermore, ADCs and CMOS logic make a coherent  $100$ -GbE solution powerful, but also power-greedy. On the other hand, DQPSK technology consumes less power, is simpler and fairly mature. In this paragraph, we want to demonstrate robust reception of a  $100$ -GbE signal based on PDM-return to zero (RZ)-DQPSK with endless optical polarization control.

The transmitter is based on a standard nested Mach–Zehnder configuration followed by an RZ modulator. The driving signals for the inphase ( $I$ ) and quadrature ( $Q$ ) component at  $28 \text{ Gb/s}$  are generated from a single  $2^{11} - 1$  pattern with a relative delay of  $51 \text{ b}$  to obtain a fairly even distribution of symbol transitions and a smooth optical spectrum. Due to the programming restrictions of the bit error ratio tester, the pattern length was limited to  $2^{11} - 1$ . The relative phase of  $90^\circ$  between  $I$  and  $Q$  in the nested modulator is stabilized by an automatic control loop. To generate the  $112$ -Gb/s polarization-multiplexed RZ-DQPSK signal, two copies of the  $56$ -Gb/s signals are added precisely bit-aligned in a polarization beam combiner with a relative delay of  $10.7 \text{ ns}$ . Noise for OSNR adjustment is added after the polarization scrambler.

At the receiver side, the signal should be split two ways, with each branch tracking one polarization channel (only one branch is implemented in the setup of Fig. 8). Independent polarization controllers can remove polarization dependent loss (PDL) limitations of a single-splitter approach. A  $\text{LiNbO}_3$  polarization controller transforms the signal so that the unwanted polarization channel is suppressed in a subsequent polarizer.

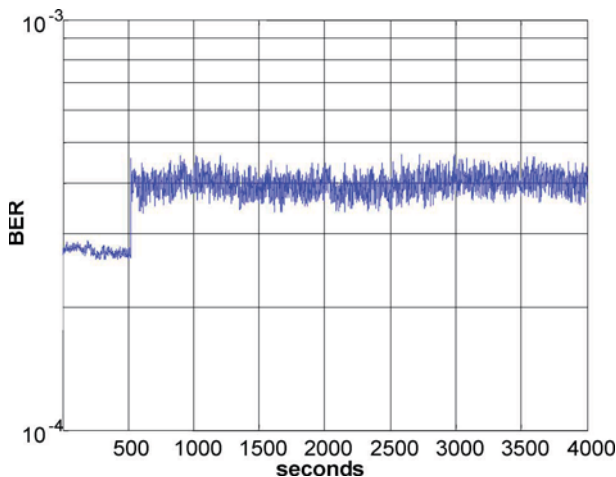


Fig. 9. Bit error rate (one sample per second) of received signal without scrambling (left part) and with a polarization scrambling of 3.5 krad/s (right).

A 10-GHz photoreceiver and a subsequent RF diode detector are used to measure the RF power carried by the optical DQPSK signal [2]. When both polarization components are present in the polarized output signal, an interference signal is generated that is pattern-dependent. The interference is present for all phase differences between the two polarization channels, since DQPSK produces symbols in four-phase states. If one polarization component is completely suppressed by the polarizer, then, the detected RF power is minimized. In fact, if RZ-DQPSK is transmitted, there should only be a clock frequency component at 28 GHz, which is blocked by the limited bandwidth of the photoreceiver and RF detector. The measured RF power is  $-20$  dB·m in the best case (when the two polarizations are well aligned) and  $-11$  dB·m in the worst case (when both polarizations pass the polarizer with equal powers), with constant optical power of  $-9$  dB·m. The FPGA-based endless optical polarization controller minimizes this interference by properly setting the voltages of the  $\text{LiNbO}_3$  polarization transformer. This unit is a less advanced polarization control system that was previously used for polarization tracking at 14 krad/s [12]. It has been slowed down to 0.37 times its original speed in order to accommodate the nonperfect nature of the interference detection scheme (mainly pattern dependence). Furthermore, the control gain has been lowered, which reduces residual errors at the expense of control speed. During the last nine months, the unit was used for tests with 112-Gb/s PDM-RZ-DQPSK at Ericsson Backnang (Germany), Ericsson Genoa (Italy) [1], and Deutsche Telekom in Nuremberg (Germany) [18] without any further adjustments or fixes. Limited by the speed of an available polarization scrambler, the maximum previously demonstrated polarization-tracking speed was 0.8 krad/s [1].

For the experiments presented in this paper, a polarization scrambler was used in Ericsson premises. For experimental convenience (but without technical significance), it differs slightly from that shown in Fig. 2, which stayed at the University of Paderborn. The scrambler used at Ericsson consists of a fast rotating  $\text{LiNbO}_3$  HWP between two quartets of fiber-loop QWPs rotating at slower rates (a few Hertz). The scrambler allows

changes in the input polarization state with 3.5 krad/s on the Poincaré sphere.

After the polarization demultiplexing, controlled delay interferometers followed by balanced photodiodes serve as direct detection receivers for I and Q signals.

The results of bit error rate measurements on the test setup during about 1 h are shown in Fig. 9. Fast scrambling at 3.5 krad/s does increase the error rate only slightly from  $3 \times 10^{-4}$  to  $4 \times 10^{-4}$ , with a slightly higher fluctuation. The observed degradation amounts to a penalty of about 0.3 dB. The operation of the polarization controller is completely unproblematic and stable. To our knowledge, this is the highest demonstrated polarization-tracking speed in any direct-detection PDM transmission experiment.

## VI. DISCUSSION AND CONCLUSION

By doubling the clock speed of the DACs and ADC and thereby broadening the polarization dither spectrum, the system is now capable of tracking arbitrary endless polarization changes up to 56 krad/s in 30-min experiments with RIE bounded below 1%, corresponding to a polarization error of 0.2 rad. This upper limit of RIE is also kept during a long-term experiment over  $>14$  days at up to 50 krad/s. The tracked polarization trajectory is calculated to be 50 Gigaradian. Power consumption of the electrode voltage sources remained  $\sim 5$  W. This can be further reduced, especially if required speed is not extreme. Additionally, the demultiplexing of a 112-Gb/s PDM-RZ-DQPSK signal scrambled at 3.5 krad/s was demonstrated with a penalty of about 0.3 dB. The bitrate transparency of optical polarization control recommends this technology also for higher symbol rates.

## REFERENCES

- [1] H. Wernz, S. Bayer, B.-E. Olsson, M. Camera, H. Griesser, C. Fuerst, B. Koch, V. Mirvoda, A. Hidayat, and R. Noé, "112 Gb/s PolMux RZ-DQPSK with fast polarization tracking based on interference control," presented at the OFC/NFOEC 2009, San Diego, CA, Mar. 22–26, Paper OTuN4.
- [2] S. Bhandare, D. Sandel, B. Milivojevic, A. Hidayat, A. A. Fauzi, H. Zhang, S. K. Ibrahim, F. Wüst, and R. Noé, "5.94-Tb/s 1.49-b/s/Hz ( $40 \times 2 \times 2 \times 40$  Gb/s) RZ-DQPSK polarization-division multiplexed C-band transmission over 324 km," *IEEE Photon. Technol. Lett.*, vol. 17, no. 4, pp. 914–916, Apr. 2005.
- [3] M. Yagi, S. Satomi, and S. Ryu, "Field trial of 160-Gbit/s, polarization-division multiplexed RZ-DQPSK transmission system using automatic polarization control," presented at the OFC/NFOEC 2008, San Diego, CA, Feb. 24–28, Paper OThT7.
- [4] T. Ito, S. Fujita, E. T. de Gabory, and K. Fukuchi, "Improvement of PMD tolerance for 110 Gb/s pol-mux RZ-DQPSK signal with optical pol-dmux using optical PMD compensation and asymmetric symbol-synchronous chirp," presented at the OFC/NFOEC 2009, San Diego, CA, Mar. 22–26, Paper OThR5.
- [5] P. Krummrich, "Field trial results on statistics of fast polarization changes in longhaul WDM transmission systems," presented at the OFC/NFOEC 2005, Anaheim, CA, USA, Mar. 6–11, Paper OThT6.
- [6] E. Bradley, E. Miles, B. Loginov, and N. Vu, "Polarization control with piezoelectric and  $\text{LiNbO}_3$  transducers," *Fiber Integr. Opt.*, vol. 21, pp. 75–104, 2002.
- [7] M. Reimer, D. Dumas, G. Soliman, D. Yevick, and M. O'Sullivan, "Polarization evolution in dispersion compensation modules," presented at the OFC/NFOEC 2009, San Diego, CA, Mar. 22–26, Paper OWD4.
- [8] R. Noé, H. Heidrich, and D. Hoffmann, "Endless polarization control systems for coherent optics," *J. Lightw. Technol.*, vol. 6, no. 7, pp. 1199–1208, Jul. 1988.

- [9] R. Noé, B. Koch, V. Mirvoda, A. Hidayat, and D. Sandel, "38 krad/s, 3.8 Gigaradian, broadband endless optical polarization tracking using LiNbO<sub>3</sub> device," *IEEE Photon. Technol. Lett.*, vol. 21, no. 17, pp. 1220–1222, Sep. 1, 2009.
- [10] F. Heismann and M. S. Whalen, "Fast automatic polarization control system," *IEEE Photon. Technol. Lett.*, vol. 4, no. 5, pp. 504–505, May 1992.
- [11] X. Zhang, G. Fang, X. Zhao, W. Zhang, L. Xi, Q. Xiong, and X. Li, "A novel endless polarization stabilizer with the additional function of stable SOP transformation in optical fiber communications," presented at the OFC/NFOEC 2009, San Diego, CA, Mar. 22–26, Paper JWA23.
- [12] B. Koch, A. Hidayat, V. Mirvoda, H. Zhang, D. Sandel, and R. Noé, "Robust, wavelength and temperature-insensitive 14 krad/s endless polarization tracking over 2.5 Gigaradian," presented at the OFC/NFOEC 2009, San Diego, CA, Mar. 22–26, Paper JThA63.
- [13] R. Noé, D. Sandel, and V. Mirvoda, "PMD in high-bitrate transmission and means for its mitigation," *IEEE J. Sel. Topics Quantum Electron.*, vol. 10, no. 2, pp. 341–355, Mar./Apr. 2004.
- [14] N. G. Walker and G. R. Walker, "Polarization control for coherent communications," *J. Lightw. Technol.*, vol. 8, no. 3, pp. 438–458, Mar. 1990.
- [15] A. Hidayat, B. Koch, H. Zhang, V. Mirvoda, M. Lichtinger, D. Sandel, and R. Noé, "High-speed endless optical polarization stabilization using calibrated waveplates and field-programmable gate array-based digital controller," *Opt. Exp.*, vol. 16, no. 23, pp. 18984–18991, 2008.
- [16] D. Sandel, F. Wüst, V. Mirvoda, and R. Noé, "Standard (NRZ 1 × 40 Gbit/s, 210 km) and polarization multiplex (CS-RZ, 2 × 40 Gbit/s, 212 km) transmissions with PMD compensation," *IEEE Photon. Technol. Lett.*, vol. 14, no. 8, pp. 1181–1183, Aug. 2002.
- [17] Two-lobed optical spectrum, indicating two optical carriers for a total of 112 Gb/s. (2008, Dec. 18). [Online]. Available: <http://www.youtube.com/watch?v=zEUDiRWNmII>
- [18] H. Wernz, S. Herbst, S. Bayer, H. Griesser, E. Martins, C. Fuerst, B. Koch, V. Mirvoda, R. Noé, A. Ehrhardt, L. Schuerer, S. Vorbeck, M. Schneiders, D. Breuer, and R. P. Braun, "Nonlinear behaviour of 112 Gb/s polarisation-multiplexed RZ-DQPSK with direct detection in a 630 km field trial," presented at the ECOC 2009, Vienna, Austria, Sep. 20–24, Paper Tu3.4.3.



**Benjamin Koch** (S'08) was born in Gutweiler, Germany, in 1977. He received the Dipl.Ing. degree in electrical engineering from the University of Paderborn, Paderborn, Germany, in 2007.

Since 2007, he has been with the University of Paderborn, where he has been involved in the research in the group of Prof. R. Noé. His research interests include optical polarization control systems.

**Vitali Mirvoda** was born in Taganrog, Russia, in 1974. He received the M.S. degree in electrical engineering from Taganrog State University of Radio Engineering, Taganrog, Russia, in 1996, and the Dr.Ing. degree from the University of Paderborn, Paderborn, Germany, in 2008.

Since 1998, he has been engaged in research on research and engineering of optical communication systems at the University of Paderborn, where he is currently a Postdoctoral Researcher in the Department of Optical Communication and High-Frequency Engineering. His research interests include polarization-mode dispersion compensation and chromatic dispersion.

**Helmut Grießer** (S'99–M'07) received the Dipl.Ing. degree in electrical engineering, in 1996 and the Ph.D. degree with a thesis on coding theory, in 2003, both from the University of Ulm, Ulm, Germany.

He joined Marconi Communications in 2002, where he was engaged in developing optical fiber communication systems. Since 2007, he has been with Ericsson GmbH, Backnang, Germany, where he has been involved in the research on high-speed optical transmission. His research interests include novel modulation formats, digital signal processing, and forward error correction for fiber communications.

**Horst Wernz** received the M.S. degree in electrical engineering from Darmstadt University of Technology, Darmstadt, Germany, in 1977 with the main focus on signal transmission in the GHz range.

During the first years, he was at AEG Telefunken, Backnang, Germany developing front-end modules for analog TV optical signal transmission. In 1999, he joined Infineon Technologies, Munich, Germany, where he was engaged in IC design for high-speed signal processing and regeneration. In 2002, he joined Marconi Communications Ondata GmbH, Backnang, Germany, where he was engaged in a funded research project for tolerant optical fiber transmission technology. He is currently with Ericsson GmbH, Backnang, where he is engaged in research on technologies for 100 Gb optical fiber transmission. His research interests include the limits of high-frequency electronics, IC design, and solving challenges of high-speed optical transmission.

**David Sandel** was born in Wangen/Allgäu, Germany, on December 26, 1966. He received the Dipl.Ing degree from the Technische Hochschule Karlsruhe, Karlsruhe, Germany, in 1992, and the Dr.Ing. degree from the University of Paderborn, Paderborn, Germany, in 1997.

Since 1997, he has been in the Department of Optical Communication and High-Frequency Engineering, University of Paderborn. His doctoral work was on fiber Bragg gratings. His current research interests include polarization-mode dispersion compensation and polarization multiplex data transmission.



**Reinhold Noé** (M'93–SM'09) was born in Darmstadt, Germany, in 1960. He received the Dipl.Ing. and Dr.Ing. degrees in electrical engineering from Technische Universität München, Munich, Germany, in 1984 and 1987, respectively.

At that time, he realized the first endless polarization control systems. Then he spent a postdoctoral year with Bellcore, Red Bank, NJ, where he continued to work on coherent optical systems. In 1988 he joined Siemens Research Laboratories, Munich. Since 1992, he has been Chair of Optical Communication and High-Frequency Engineering, University of Paderborn, Germany. Most of his recent experiments deal with high-speed endless optical polarization control and realtime synchronous QPSK transmission. He has (co)authored more than 200 journal and conference publications.